Bulk and surface properties of hexagonal-close-packed Be and Mg

2001 J. Phys.: Condens. Matter 13 10767

(http://iopscience.iop.org/0953-8984/13/48/303)

INSTITUTE OF PHYSICS PUBLISHING JOURNAL OF PHYSICS: CONDENSED MATTER

J. Phys.: Condens. Matter **13** (2001) 10767–10776 PII: S0953-8984(01)26953-7

Bulk and surface properties of hexagonal-close-packed Be and Mg

E Wachowicz and A Kiejna

Institute of Experimental Physics, University of Wrocław, Plac M Borna 9, 50-204 Wrocław, Poland

Received 12 July 2001, in final form 3 October 2001
Published 16 November 2001

Abstract

Density functional theory and a plane-wave basis pseudopotential technique are applied to calculate the bulk and the (0001) surface properties of hexagonal-close-packed (hcp) beryllium and magnesium. The calculations were performed with two forms of the exchange–correlation functional. The bulk properties of the two metals calculated within the generalized gradient approximation (GGA) are closer to the measured ones than the local density approximation (LDA) results are. The GGA also provides results for lattice relaxations, work functions, and surface energies which are in a better agreement with experimental values than the LDA results are. The changes of surface energy and work function with slab thickness varying between 3 and 13 atomic layers were considered. Quantum-size effects did not influence the calculated work function and surface energies significantly.

1. Introduction

First-principles calculations allow one to study different complex systems of many atoms. But even for relatively simple and well-known systems, there are still some interesting questions remaining open. One such question concerns the proper description of the exchange–correlation interaction. It is generally assumed that the local density approximation (LDA) describes the properties of bulk metals and the clean metal surfaces well. However, there are quite a few situations where LDA leads to inaccurate results. For example, it is well known that LDA overestimates the bonding strength and the bulk modulus in some metals (e.g. aluminium, transition metals). These deficiencies can normally be remedied by employing the generalized gradient approximation (GGA) to the exchange–correlation functional instead of the LDA. In this paper we present the results of a systematic and comparative study of the bulk and surface properties of hcp Mg and Be performed within the LDA and the GGA. We are interested in the extent to which the GGA improves the calculated structural and binding properties of the two metals over the LDA results.

Beryllium and magnesium crystals have the same hcp structure but differ in the extent of the contraction of their c/a ratio with respect to the ideal one. They are characterized by closed ns^2 shells, and have the same valency, but there are no p electrons in Be. They differ

0953-8984/01/4810767+10$30.00

also in some other electronic properties: Mg is almost free-electron-like whereas Be, although in general metallic, shows a low density of states at the Fermi energy, and thus exhibits some features of covalent-like bonding. This covalent-like character of the bonding has also been revealed at the Be($10\bar{1}0$) surface by recent calculations of surface core-level shifts (SCLSs) [1]. On the other hand, the SCLS at Be(0001) changes very little with relaxation [2, 3], suggesting a free-electron-like character of the bonding at this surface. This was also confirmed by the recent attempt to explain the outward relaxation of the topmost layers observed at Be(0001) and Mg(0001) surfaces as resulting from the accumulation/depletion of the electron charge due to the long-range Friedel oscillations [4]. In this paper we provide the results of more extensive calculations for these metals. The convergence of the electronic characteristics of surfaces—work function and surface energy—was examined for (0001) metal surfaces represented by slabs of thickness up to 13 atomic layers.

The method and computational details are briefly discussed in section 2. Section 3 presents the results and a discussion, and section 4 summarizes the conclusions.

2. Method

The calculations reported in this work were performed with the fhi96md program package [5] based on density functional theory (DFT) and the plane-wave-basis pseudopotential method. The exchange–correlation energy was calculated within the LDA using the Perdew–Zunger parametrization [6, 7]. For the GGA calculations the Perdew–Wang form [8] was employed. To represent the electron–ion interaction, fully separable non-local pseudopotentials [9] were applied, taking into account the correction for non-linear exchange–correlation interaction between the core and the valence electrons. The electronic wave functions were expanded in a plane-wave basis set with a kinetic energy cut-off equal to 30 Ryd. The $\boldsymbol{k}$-space integration was performed according to the Monkhorst–Pack scheme [10]. For the bulk crystal calculations, 150 special $\boldsymbol{k}$-points in the irreducible wedge of the Brillouin zone (BZ) were used, while in the surface calculations 42 $\boldsymbol{k}$-points were used. The quality of integration was improved by using the Fermi surface smearing of 0.1 eV.

In calculating the surface properties of the hcp (0001)-oriented metals, a supercell geometry was applied. The crystal surface was represented by slabs consisting of several atomic layers separated by vacuum regions. Every atomic layer was represented by a single atom. The thicknesses of both crystal and vacuum regions were chosen large enough to avoid interaction between the surfaces of neighbouring slabs. Good convergence in the calculated total energies was obtained for slabs eleven atomic layers thick for both elements (19 Å for Be and 28 Å for Mg) and a vacuum region thickness of about 10 Å for Be and 18 Å for Mg. To account for the lattice relaxations, the positions of atoms in the three topmost layers (on one side of the slab) were optimized until the sum of the forces on each atom was smaller than 0.01 mRyd Bohr^{-1}. The artificial electric field arising on the other side of the slab was compensated by the dipole correction [11].

3. Results

3.1. Bulk properties

In the calculations of the bulk properties of the hcp crystals, the crystals were modelled by hexagonal supercells containing two atoms. Table 1 presents results for the equilibrium bulk binding properties calculated by minimization of the total energy for two approximations applied to the exchange–correlation energy functional. Zero-point vibrations were not taken into account. To obtain the minimum-energy lattice parameters, the total energies were calculated for different pairs of a and c/a. These energies were then fitted to the 2D cubic polynomial

$$E(x, y) = c_0 + c_1x + c_2y + c_3x^2 + c_4y^2 + c_5xy + c_6x^2y + c_7xy^2 + c_8x^3 + c_9y^3 \qquad (1)$$

where x denotes the lattice constant a, y denotes the c/a ratio, and the c_i are parameters to be determined from the fit. Using this energy expression, the minimum energy was found for the values of a and c/a given in table 1. The results obtained agree very well with the experimental data. For beryllium the lattice constant $a = 2.231$ Å calculated within the LDA is lower by 2.6% than the measured value. Similarly, for Mg the calculated LDA lattice constant $a = 3.127$ Å is underestimated by 2.6%. This underestimation of the lattice constant by the LDA is greatly reduced by applying the GGA for both Be and Mg. It is also seen that the two approximations give a contracted c/a ratio for Mg and a slightly expanded c/a for Be. The cohesive energy and the bulk modulus corresponding to these structures are also presented in table 1. The cohesive energy was calculated as a difference between the total energy per atom in a bulk crystal and the total energy of a free atom. The latter was determined for a single atom in a cubic cell of box length about 10 Å that was big enough to avoid interactions with atoms from the neighbouring cells, using the Γ point for the $\boldsymbol{k}$-space integration and with the energy cut-off equal to 20 Ryd. Though one usually performs the total-energy calculation of a

Table 1. Calculated physical properties of hcp beryllium and magnesium crystals at 0 K.

Reference	Lattice constant a (Å)	Lattice constant c/a	Cohesive energy (eV)	Bulk modulus (GPa)
Be				
This work, LDA	2.23	1.573	4.20	128
This work, GGA	2.26	1.570	3.74	115
Other calculations, LDA[a]	2.25	1.586	3.60	131
LDA[b]	2.23	1.566	4.35	135.6
LDA[c]	2.23	1.580	4.08	140
Other calculations, GGA[c]	2.25	1.570	3.65	120
Experiment[d]	2.29	1.567	3.33	110
Mg				
This work, LDA	3.13	1.616	1.78	40.2
This work, GGA	3.18	1.615	1.50	35.5
Other calculations, LDA[e]	3.16	1.610	1.64	35.0
LDA[f]	3.12	1.616	—	38.4
LDA[g]	3.16	1.590	1.76	39.0
LDA[h]	3.18	1.623	—	37.7
Other calculations, GGA[g]	3.20	1.660	1.42	30.0
Experiment[d]	3.21	1.624	1.51	35.4

[a] Reference [27].
[b] Reference [28].
[c] Reference [29].
[d] Reference [30].
[e] Reference [31].
[f] Reference [22].
[g] Reference [32].
[h] Reference [23].

free atom with the cut-off energy the same as in the bulk calculation, in this case convergence tests showed that the total-energy change on increasing the cut-off from 15 Ryd to 20 Ryd was less than 0.02 eV for both metals and approximations, so the latter one yields well-converged results. The LDA overestimates the cohesive energy for Be and Mg compared to experiment. The use of the GGA reduces its values for both metals. The agreement between calculated and experimental values of the cohesive energy could be further improved by considering the spin polarization of the free atom. The atomic spin-polarization correction which lowers the cohesive energy was not taken into account in this work. The bulk modulus was calculated by fitting the energy versus volume curve to the Murnaghan equation of state [12]. The values calculated within the LDA are larger by 16% (Be) and 13% (Mg) than the measured ones. The GGA reduces the bulk modulus for both metals and brings it into very good agreement with the experimental data. So the improvement of the results for the bulk binding properties caused by the application of the GGA is clearly visible. The calculated lattice parameters of table 1 were used as input parameters for surface calculations.

3.2. Surface properties

The calculations performed for eleven-layer-thick Be and Mg films led to well-converged results for surface lattice relaxations for both metals. Table 2 compares the calculated relaxations of the three topmost layers with the experimental data. In reference [4] the observed relaxation pattern was explained on the basis of the analysis of the calculated electron-charge-density distribution perpendicular to the surface. It was found that the Friedel oscillations in the surface electron-density distribution in the direction perpendicular to the metal surface are responsible for the electrostatic forces making the topmost atomic layers repel one another. The same mechanism is valid in the case of both Be(0001) and Mg(0001) surfaces, indicating free-electron-like character of the bonding [4].

Table 2. Multilayer relaxations $\Delta_{ij} = (d_{ij} - d)/d$ of surface layers i and j (in % of the interlayer spacing d in the bulk) for the (0001) surfaces of Be and Mg.

Surface	Δd_{12}	Δd_{23}	Δd_{34}	Reference
Be(0001)	2.74	1.18	0.77	LDA
	3.17	1.15	0.65	GGA
	5.8	−0.2	0.2	Experiment (300 K)[a]
	3.1	1.4	0.9	Experiment (100 K)[b]
	2.4			Experiment (0 K)[c]
Mg(0001)	1.13	0.31	0.21	LDA
	2.04	1.13	0.72	GGA
	1.9	0.8	−0.4	Experiment (100 K)[d]
	1.7			Experiment (0 K)[a]

[a] Reference [33].
[b] Reference [34].
[c] Reference [35].
[d] Reference [36].

In order to extract the well-converged values of the electronic surface characteristics corresponding to semi-infinite samples, the evolutions of the work function and surface energy with increasing slab thickness were examined. In the calculations the slab thickness varied from three to thirteen atomic layers and the three topmost metal layers were allowed to relax.

The work function was calculated from the standard expression

$$\Phi = V_{vac} - E_F \tag{2}$$

where V_{vac} is the electrostatic potential in the vacuum region and E_F is the Fermi energy of the slab. For both exchange–correlation energy approximations applied, the work-function changes were calculated for relaxed and unrelaxed surfaces. The variation of the work function with slab thickness for Be(0001) and Mg(0001) is presented in figures 1 and 2. Since there were actually no differences between the results for relaxed and unrelaxed surfaces, only the former are displayed in the figures. As is seen for beryllium, the LDA and GGA work functions differ systematically by about −0.25 eV. The work functions increase by about 0.1 eV (LDA) and 0.06 eV (GGA) for slab thickness increasing from three to five monolayers, then converge to 5.57 eV (LDA) and 5.36 eV (GGA). The uncertainty range in the convergence of the work function for slabs thicker than five atomic layers is smaller than 0.04 eV. For the Mg(0001) surface (figure 2) the work function experiences the same kinds of change for both LDA and GGA with increasing slab thickness: for thin slabs the work function decreases by about 0.1 eV, reaches a shallow minimum of 3.86 eV (LDA) and 3.72 eV (GGA) for slab thicknesses of 7–8 monolayers and saturates at the thickness of 10–12 layers. The uncertainty in the determination of Φ, for slabs thicker than six atomic layers, is smaller than 0.03 eV. The GGA rigidly shifts the LDA work functions downward by about 0.15 eV. They converge to the values of 3.88 eV (LDA) and 3.74 eV (GGA). The convergence of the work-function values could be improved even further by applying, instead of equation (2), a classical definition of the work function using the electrostatic potential step at the surface and the Fermi energy determined for a bulk crystal [13] instead of that for a film. The latter definition allows one to eliminate the influence of the quantum-size effect (QSE). The QSE, however, appears to be very small for Be(0001) and Mg(0001) slabs as discussed below.

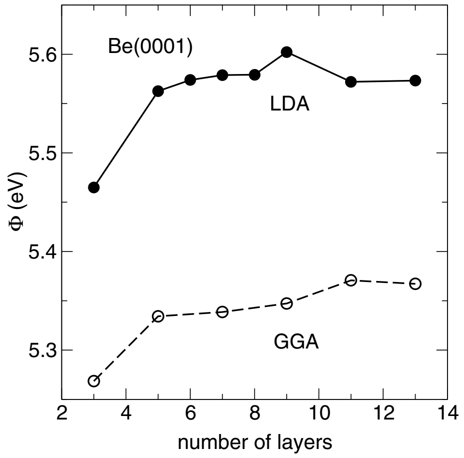

Figure 1. Variation of the calculated work function of Be(0001) with slab thickness.

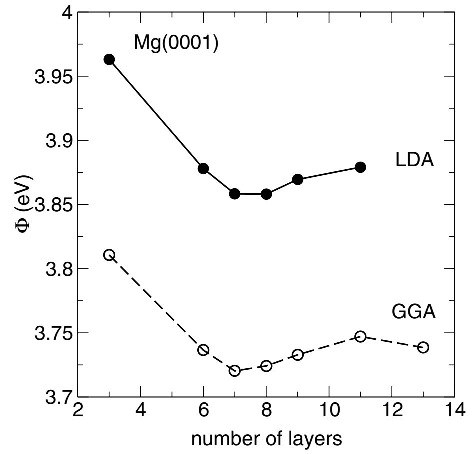

Figure 2. Variation of the calculated work function of Mg(0001) with slab thickness.

Table 3 compares the calculated work functions for eleven-monolayer-thick (0001)-oriented slabs with experimental data and results of previous calculations. The calculated LDA work function of the Be(0001) surface, similarly to in previous LDA calculations [14], is about 0.5 eV higher than the measured value. The GGA value is shifted down to closer to the measured one [15]. The difference (0.26 eV) is not big and moreover the authors of the experimental paper stated that the actual work function should be slightly higher. In the case of Mg(0001) the LDA work function is a little closer to the measured value [16] than that provided by the GGA, but both are within 0.08 eV of the experimental one.

Table 3. Calculated work functions and surface energies of the (0001) surfaces of Be and Mg compared with other calculations and experimental results.

Surface	Φ (eV)	σ (eV/atom)	Reference
Be(0001)	5.57	0.54	This work, LDA
	5.36	0.46	This work, GGA
	5.54[a]	0.52 [a]	Other calculations, LDA
	5.1[b]	0.31[c]	Experiment
Mg(0001)	3.88	0.35	This work, LDA
	3.76	0.30	This work, GGA
	3.69[d]	0.337[e], 0.319[f]	Other calculations, LDA
	3.84[g]	0.28[b]	Experiment

[a] Reference [14].
[b] Reference [15].
[c] Reference [21].
[d] Reference [37].
[e] Reference [22].
[f] Reference [23].
[g] Reference [16].

The reduced GGA work functions, relative to the LDA ones, reflect the lower electron charge density due to the increased volume of the GGA unit cell for the two metals. The average electron densities for the bulk Be crystal are equal to 0.0392 electron Bohr^{-3} (LDA) and 0.0377 electron Bohr^{-3} (GGA) whereas for the bulk Mg they amount to 0.0138 electron Bohr^{-3} (LDA) and 0.01315 electron Bohr^{-3} (GGA). They should also correspond to a diminished surface dipole moment of the electron-density distribution. Figures 3 and 4 display the electron-density-difference contours at the relaxed Be(0001) and Mg(0001) surfaces, respectively. The lines represent the difference between the average valence electron charge density in the bulk crystal and the electron-charge-density distribution in the surface region.

For both metals a spreading of the electronic charge in the surface region can be noticed. In the case of Be the electron-density contours calculated within the GGA show bigger changes between the constant-density lines than those calculated within the LDA. This is in contrast to the case for the Mg(0001) surface where the LDA leads to bigger changes in the charge-density distribution than the GGA.

Another important surface quantity is the surface energy σ, which for an n-layer slab is usually determined from the relation

$$\sigma(n) = \frac{1}{2}(E_n - nE_B) \tag{3}$$

where E_n is the total energy per unit cell of the n-layer slab and E_B is the total energy per layer of an infinite bulk crystal. The factor 1/2 accounts for the two surfaces of the slab. For a sufficiently large number of layers, $\sigma(n)$ calculated from (3) should converge to the surface energy of a semi-infinite sample. However, it was pointed out [17] that surface energy will diverge with slab thickness because the total energy E_B calculated for a bulk system is not exactly equal the slope of the slab energy versus n [17,18]. In order to achieve stable, convergent results for surface energies, some other methods were suggested [17–19] which modify the original equation (3). In one of the modifications [18], the surface energy is calculated from the formula

$$\sigma(n) = \lim_{n\to\infty} \frac{1}{2}\left(E_n - \frac{n}{n_B}E_{n_B}^{full}\right) \tag{4}$$

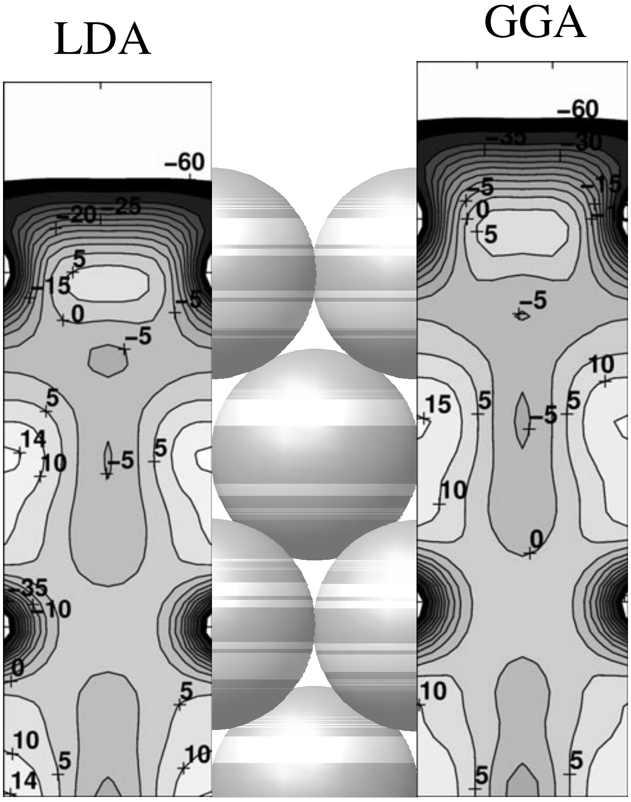

Figure 3. The charge-density distribution near the relaxed Be(0001) surface cut along the $(10\bar{1}0)$ plane. The atomic configuration commensurate with the optimized positions calculated in the LDA is also shown. Electron-density-difference distributions are shown relative to the average electron density in the bulk expressed as a percentage of the latter. Darker grey is used to indicate regions with smaller charge density while lighter shades represent regions with charge density above average. For the density distribution, only charge of the valence electron is shown; therefore the circular regions of lowest charge density observed at the sides represent atom positions cut by the chart plane.

where $E_{n_B}^{full}$ is the total energy of the bulk supercell of n_B atoms with the vacuum region filled with atoms. For this approach, in our calculations we used $n_B = n + 7$, with n ranging from three up to thirteen.

A different method of avoiding the divergence problem was suggested by Boettger [17]. For a sufficiently thick slab, the total binding energy E_B can be extracted from the linear dependence of E_n on E_B that is obtained from the inversion of equation (3). By making a linear fit to the total energy of the slab as a function of n, and calculating its slope, one gets the value of E_B which can in turn be used to calculate the surface energy of a particular slab from equation (3).

The variations of the surface energy versus the slab thickness of the relaxed (0001) surfaces of Be and Mg calculated using different approaches are presented in figures 5 and 6, respectively. Interestingly, in the case of the Mg(0001) surface (figure 6) the surface energy calculated from the original expression (3) converges very well, whereas for the Be(0001), as for other metal surfaces [17–20], it diverges linearly with increasing slab thickness (figure 5). At this stage, the reason for this unusual behaviour for the Mg(0001) surface is not clear to us

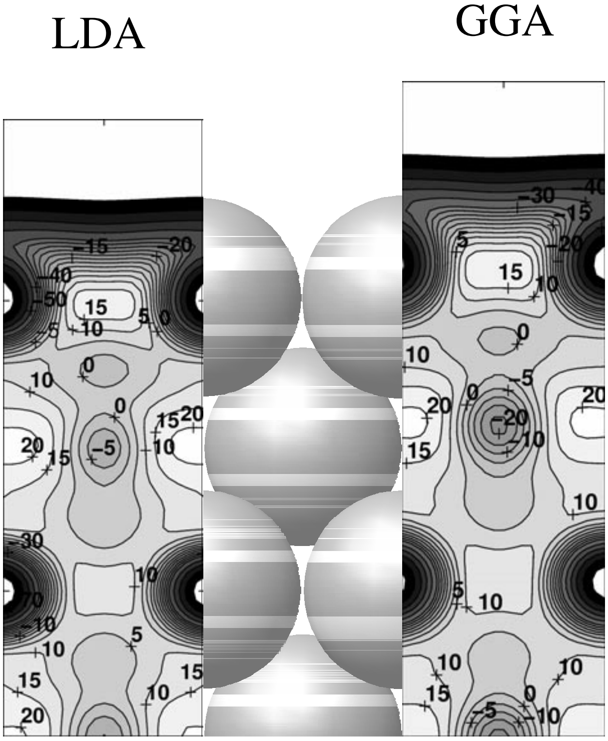

Figure 4. As figure 3, but for the Mg(0001) surface.

and is currently being investigated.

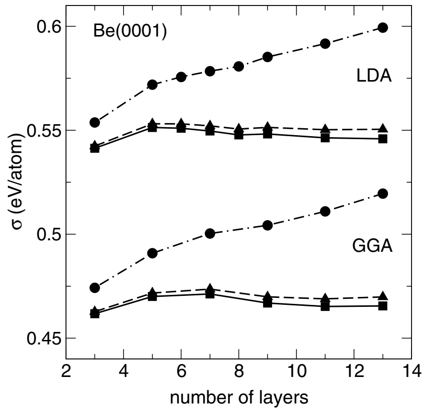

Figure 5. Calculated surface energies for Be(0001) as functions of slab thickness. The surface energy was calculated according to: (●) equation (3); (▲) equation (4); (■) linear regression.

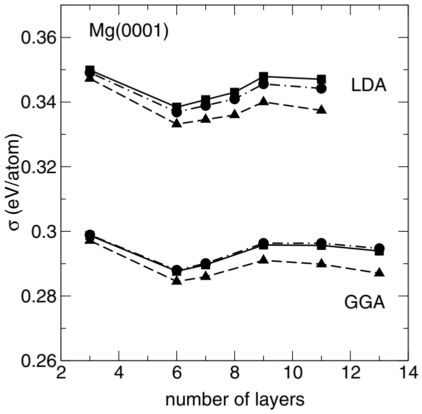

Figure 6. Calculated surface energies for Mg(0001) as functions of slab thickness. The surface energy was calculated according to: (●) equation (3); (▲) equation (4); (■) linear regression.

For Be(0001) the calculated surface energy shows the same character of changes with slab thickness for the LDA as for the GGA. Similarly, as for the work function, the GGA rigidly shifts the LDA surface energy downward, by 0.8 eV/atom for Be(0001) and 0.05 eV/atom for

Mg(0001). Results obtained with equation (4) and with the help of linear regression differ only slightly, and for thicker slabs the calculated surface energy actually does not change with the slab thickness. The calculated surface energy of Be(0001) corresponding to semi-infinite samples is equal to 0.54 eV/atom (LDA) and 0.46 eV/atom (GGA). These values are higher than the experimental surface energy of 0.31 eV/atom [21], though the agreement of the GGA result is much improved.

In contrast to the case for the Be(0001) surface, for the Mg(0001) surface the curves representing the variation of the surface energy versus slab thickness calculated according to equations (3) and (4), and from equation (3) with E_B determined from the linear regression, are very alike (figure 6) and do not undergo significant changes. The surface energy converges to 0.35 eV/atom (LDA) and 0.30 eV/atom (GGA), which can be considered as corresponding to values for semi-infinite samples. In view of the experimental uncertainties, these results agree very well with the measured value of 0.28 eV/atom [21]. Again the GGA surface energy is superior compared with LDA results from this and previous calculations [22, 23] (table 3).

The variations of the surface energy as well as of the work function versus the slab thickness that are displayed in figures 1, 2 and figures 5, 6 have a rather smooth character, thus showing the very small influence of the quantum-size effect [24] which should be manifested in oscillations of surface quantities as a function of the varying thickness of the slab. The QSE that results from the size-dependent quantization of the electron states in the direction perpendicular to the surface being different from that for the bulk was confirmed also for crystalline Al(111), Al(110), and Mg(0001) slabs [17,20,25,26]. The work-function variations reported in reference [25] for the ideal Mg(0001) surface, and ascribed to the QSE, are of similar magnitude (~0.1 eV) to those reported in this work, and are smaller than those for Al surfaces [17, 20]. This smaller amplitude for lower-density metals is in agreement with the prediction of the theory [24]. On the other hand, for Be(0001) and Mg(0001), the work-function and surface energy variations do not show any regular period of oscillations, which for the jellium is predicted [24] to be an integral multiple of half of the Fermi wavelength of the given metal. In the crystalline calculations the thickness of the slab can change only by integral numbers of layers, so the oscillations could be eliminated by incoherent changes of the thickness. Also, the oscillatory character of the lattice relaxation of extension/contraction type [4] could contribute to the reduction of the QSE oscillations at the surfaces considered.

4. Summary

We have performed extensive first-principles calculations of the structural and electronic properties for the bulk and the clean (0001) surfaces of Be and Mg. For both metals the lattice constants, bulk moduli, and cohesive energies calculated within the GGA are superior to the LDA results and show better agreement with experiment. The first three interlayer spacings were found to expand. The magnitudes of the relaxations of the topmost layers calculated with the LDA are underestimated compared with measurements. Good agreement was found between measured relaxations and those calculated with the GGA for both metal surfaces, although the latter are still bigger than the experimental ones. As for the surface energy and work function, GGA calculations provide values which are in better agreement with experimental results than the LDA ones.

The variations of the work function and surface energy with slab thickness were examined. For slabs thicker than five atomic layers the changes in the work function are within 0.04 eV for Mg(0001) and 0.03 eV for Be(0001), showing no oscillatory character which could be attributed to QSE. The well-converged results obtained for the surface energy are in very good agreement with the measured values.

Acknowledgment

One of us (EW) was supported by grant No 2016/W/IFD/2000 from the University of Wrocław.

References

[1] Cho J-H, Kim K S, Lee S-H, Kang M-H and Zhang Z 2000 *Phys. Rev.* B **61** 9975

[2] Alden M, Skriver H L and Johansson B 1993 *Phys. Rev. Lett.* **71** 2457

[3] Feibelman P J and Stumpf R 1994 *Phys. Rev.* B **50** 17 480

[4] Wachowicz E and Kiejna A 2000 *Solid State Commun.* **116** 17

[5] Bockstedte M, Kley A, Neugebauer J and Scheffler M 1997 *Comput. Phys. Commun.* **107** 187

[6] Ceperley D M and Alder B J 1980 *Phys. Rev. Lett.* **45** 567

[7] Perdew J P and Zunger A 1981 *Phys. Rev.* B **23** 5048

[8] Perdew J P, Burke K and Wang Y 1996 *Phys. Rev.* B **54** 16 533

[9] Troullier N and Martins J L 1991 *Phys. Rev.* B **43** 1993

[10] Monkhorst H J and Pack J D 1976 *Phys. Rev.* B **13** 5188

[11] Neugebauer J and Scheffler M 1992 *Phys. Rev.* B **46** 16 067

[12] Murnaghan F D 1944 *Proc. Natl Acad. Sci. USA* **30** 244

[13] Fall C J, Binggeli N and Baldereschi A 1999 *J. Phys.: Condens. Matter* **11** 2689

[14] Feibelman P J 1992 *Phys. Rev.* B **46** 2532

[15] Green A K and Bauer E 1978 *Surf. Sci.* **74** 676

[16] Michaelson H B 1977 *J. Appl. Phys.* **48** 4719

[17] Boettger J C 1996 *Phys. Rev.* B **53** 13 133

[18] Fiorentini V and Methfessel M 1996 *J. Phys.: Condens. Matter* **8** 6525

[19] Boettger J C, Smith J R, Birkenheuer U, Rösch N, Trickey S B, Sabin J R and Apell S P 1998 *J. Phys.: Condens. Matter* **10** 893

[20] Kiejna A, Peisert J and Scharoch P 1999 *Surf. Sci.* **432** 54

[21] Hayden B E, Schweitzer E, Kötz R and Bradshaw A M 1981 *Surf. Sci.* **111** 26

[22] Wright A F, Feibelman P J and Atlas S R 1994 *Surf. Sci.* **302** 215

[23] Ismail, Hofmann Ph, Plummer E W, Bungaro C and Kress W 2000 *Phys. Rev.* B **62** 17 012

[24] Schulte F K 1976 *Surf. Sci.* **55** 427

[25] Feibelman P J 1983 *Phys. Rev.* B **27** 1991

[26] Ciraci S and Batra I P 1986 *Phys. Rev.* B **33** 4294

[27] Chou M Y, Lam P K and Cohen M L 1983 *Phys. Rev.* B **28** 4179

[28] Pari G, Kumar V, Mookerjee A and Bhattacharyya A K 1999 *J. Phys.: Condens. Matter* **11** 4291

[29] Holzwarth N A W and Zeng Y 1995 *Phys. Rev.* B **51** 13653

[30] Ashcroft N W and Mermin N D 1976 *Solid State Physics* (New York: Holt, Rinehart and Winston)

[31] Chou M Y and Cohen M L 1986 *Solid State Commun.* **57** 785

[32] Fuchs M, Bockstedte M, Pehlke E and Scheffler M 1997 *Phys. Rev.* B **57** 2134

[33] Davis H L, Hannon J B, Ray K B and Plummer E W 1992 *Phys. Rev. Lett.* **68** 2632

[34] Pohl K, Cho J H, Terakura K, Scheffler M and Plummer E W 1998 *Phys. Rev. Lett.* **80** 2853

[35] Plummer E W 2000 private communication

[36] Sprunger P T, Pohl K, Davis H L and Plummer E W 1993 *Surf. Sci.* **297** L48

[37] Chulkov E V and Silkin V M 1986 *Solid State Commun.* **58** 273